A 64 Gb/s NRZ O-Band Ring Modulator with 3.2 THz FSR for DWDM Applications

Chuan Xie*, Mayank Raj, Anish Joshi, Zakriya Mohammed, Gareeyasee Saha, Zhaowen Wang, Parag Upadhyaya, and Yohan Frans

Advanced Micro Devices, Inc., San Jose, CA 95124, USA.

*chuan.xie@amd.com

Abstract: We demonstrate the highest BW-FSR product O-band Si microring modulator to date. The device achieves 3.2 THz FSR, 41 GHz BW, 44 pm/V modulation efficiency, and operates at 64 Gb/s NRZ. © 2024 The Author(s)

1. Introduction

To bring high-density optical IOs into the package of a high-capacity, high-bandwidth computing or switching IC (known as co-packaged optics, or CPO), photonic modulators must have a small footprint and low power consumption. Dense wavelength division multiplexing (DWDM) may also be necessary to raise the bandwidth density and reduce the optical fiber count [1]. Silicon microring or microdisk modulators (MRM or MDM) are excellent candidates for CPO because of their small size and intrinsic compatibility with DWDM [2].

In a DWDM channel plan, crosstalk between optical modulators of adjacent channels sets a lower limit on the channel spacing (CS). For a channel symbol rate of around 56 GBd, this CS lower bound is typically 200 GHz. To accommodate a 16-λ DWDM channel plan with 200 GHz channel spacing, the modulator needs a free spectral range (FSR) of 3.2 THz. However, MRMs utilize rib waveguide geometry, which is susceptible to higher propagation losses in tight bends. Because of bending loss concerns, an MRM is typically designed with a radius between 5 and 10 µm, which limits FSR in the range of 1.2–2.4 THz [2, 3].

Explored methods to achieve FSR > 2.4 THz include MDMs [4] and interior-ridge MRMs (1.75 µm–2.5 µm radius) [5] with a vertical PN junction or an interleaved junction. These designs offer a high FSR (up to 6.92 THz) but exhibit limited modulation bandwidth (< 25 GHz) and data rates (10–30 Gb/s) [6–8].

In this paper, we present the design and performance of a novel MRM with a 3.8 µm radius (FSR = 3.2 THz). The bending loss is controlled by utilizing a wider ring waveguide, and the device design is optimized to achieve a 3-dB bandwidth of over 41 GHz (with detuning at maximum modulation slope) by making use of inductive peaking. To the best of our knowledge, this is the smallest O-band MRM in a simple rib waveguide structure with a demonstrated speed of 64 Gb/s NRZ modulation.

2. Modulator Design

The MRM is designed for fabrication in the 45 nm monolithic CMOS electronic-photonic process (45CLO) [9]. The layout of the device is shown in Fig. 1.

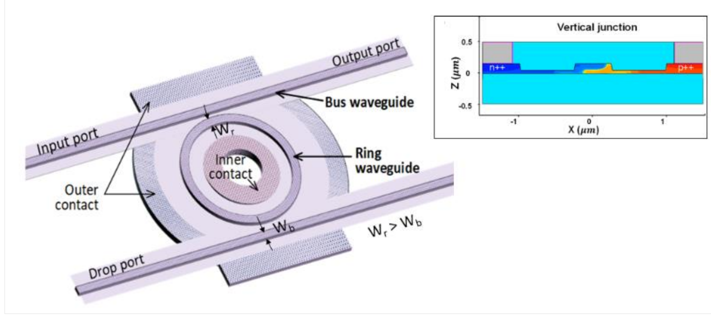

Fig. 1. MRM schematic with the cross-section of the PN junction

The ring radius is 3.8 µm to facilitate a 3.2 THz FSR. Forming such a small ring with the same waveguide width as that of the bus waveguide would result in unacceptably high bending loss. To solve this constraint, we widen the ring waveguide (W_r) while keeping the width of the bus waveguide at the cut-off of single-mode operation (W_b). Due to the small radius of the ring, W_r can be significantly larger than W_b while still maintaining single-mode operation. The wider ring waveguide also allows a wider vertical section in the carrier-depletion vertical junction design (Fig. 1), increasing the junction area that overlaps the mode to improve modulation efficiency (ME). Despite the difference in width ($W_r > W_b$), the bus-ring coupling is optimized with a gap width well over the minimum value allowed by the design rule for achieving critical coupling for a target Q factor of 4500. A 10% drop port is included, which terminates with a photodetector (not shown in Fig. 1) for tuning and locking the ring resonance (via thermal tuners, which are also not shown). The increase in RC time from the vertical junction is compensated for by inductive peaking. To accomplish the inductive peaking (350 pH) scheme, the metal traces are designed using two loop square spiral geometries between the inner (N Junction) and the high-speed driving signal. Although adjusting the wavelength detuning of a ring modulator also introduces optical peaking to extend the 3-dB roll-off frequency, using inductive peaking has no negative effect on the low-frequency response (no OMA reduction) [10].

3. Performance Data of Fabricated Device

3.1 Modulator FSR, Q-Factor, DC Extinction Ratio and Modulation Efficiency

The fabricated MRM, the metal layout for the contact traces forming an integrated inductor, the landing pad (for Electronic Integrated Circuit, or EIC), and the bond pads are shown in Fig. 2. The bond pads are designed for use with RF probes, and the heater control is for tuning the resonance of the MRM. The process specification of the multi-project wafer (MPW) silicon-on-insulator (SOI) platform can be found in ref [9]. The measured FSR of the MRM is shown in Fig. 3(a). Without biasing the heater at 0 V (PN biasing), the MRM has resonances at 1293.4 nm and 1311.7 nm, corresponding to a FSR of 18.3 nm or 3.2 THz. The transmission curves of the MRM near the 1311.7 nm resonance are shown in Fig. 3(b). The transmission loss on resonance is about 25 dB and a Q of 4500. The modulation efficiency is measured by biasing the PN junction and calculating the shift in resonance, which is found to be 44 pm/V or 7.7 GHz/V (average of parts from 10 reticle sites across the wafer).

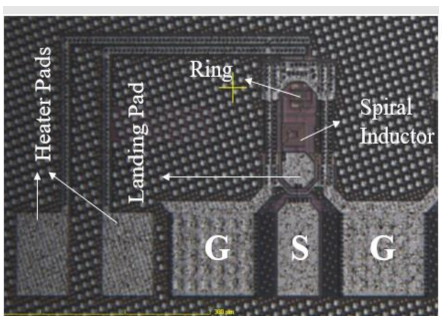

Fig. 2. Top view of the fabricated device.

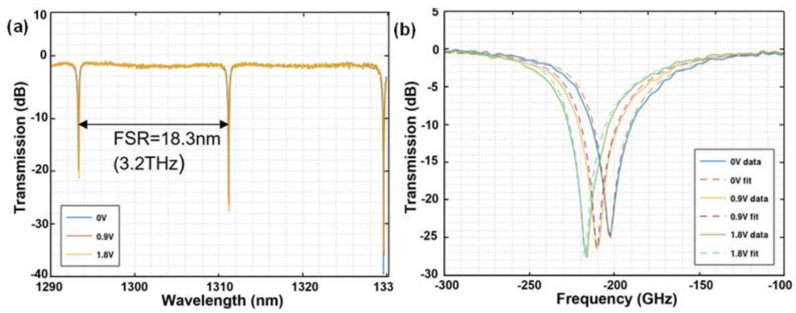

Fig. 3. Sample spectra. (a) 1290 nm to 1330 nm spectra showing FSR, (b) resonance near 1310 nm vs. bias (frequency relative to that of 1310 nm).

3.2 Modulator Bandwidth and High-Speed Experiments

To assess the effect of inductive peaking, the same microring modulator is fabricated with and without an integrated inductor. Fig. 4(a) shows representative s21 data of the proposed MRM without an inductor, while Fig. 4(b) shows s21 data with a peaking inductor. The red curves are measured at the maximum modulation slope point on the shorter wavelength side of the resonance nearest to 1310 nm. The blue and yellow curves are measured at wavelengths 25 pm below and above the maximum slope point, respectively. The raw data are fitted to a 5th-order polynomial, and the numbers in the legend are the 3 dB bandwidth (GHz) calculated from the fitted curves. The S21 data are not normalized, so the level at low frequencies of each curve is indicative of the modulation efficiency. The measurement was taken using a Lightwave Component Analyzer (LCA). The LCA was calibrated using a calibration substrate to remove the response from probes and cables. As shown, the bandwidth can be optimized to 41 GHz (an 11 GHz improvement) with inductive peaking to support high data rates.

To measure the optical eye diagrams, we used a Keysight PPG to produce the PRBS pattern. The maximum output swing of the PPG was 0.6 V_{pp}. Therefore, a 67 GHz linear amplifier from Hyper Labs plus a bias-T was used to produce 1.8 V_{pp} swing and to set proper junction bias. The modulation signal was applied to the modulator via a 67 GHz GSG probe. The eye diagrams for the electrical driving signal with the cable to the GSG probe de-embedding are shown in Figs. 4(c) and 4(d). The output of the MRM passed through a praseodymium-doped fiber amplifier (PDFA) to counter the losses of two grating couplers and a polarization synthesizer. The eye diagrams were captured at a laser detuning that produces the highest optical modulation amplitude (OMA). With a high extinction ratio (> 4.5 dB), the eye diagrams were continuously open at data rates of 53 Gb/s [Fig. 4(e)] and 64 Gb/s [Fig. 4(f)]. It is to be noted that 64 Gb/s is the highest data rate of the pattern generator used. As shown in Table 1, all the previously reported large FSR ring modulators relied on complicated geometries and had limited bandwidth. In comparison, the proposed MRM is based on a simple rib waveguide structure with the highest bandwidth (BW) FSR product to be reported in the O-band.

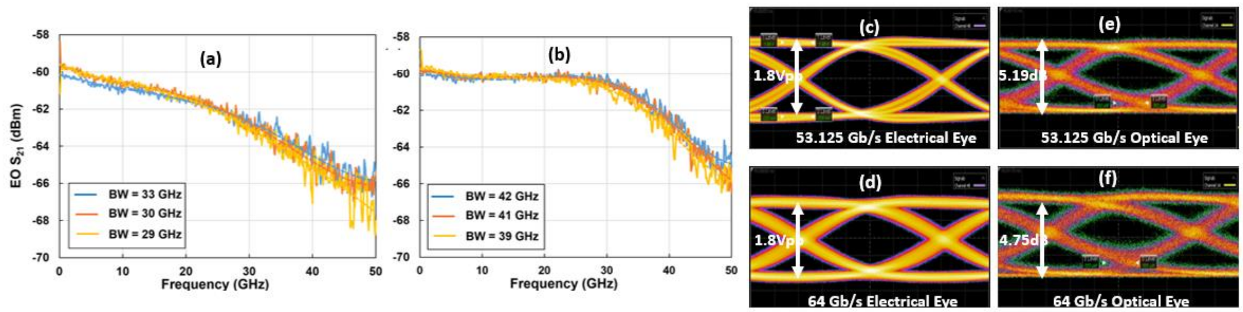

Fig. 4. EO S21 data of the proposed MRM (a) without inductor (b) with inductor. Electrical eye diagrams with GSG probe de-embedding(c) 53.125 Gb/s speed (d) 64 Gb/s speed. Optical eye diagrams with (e) 53.125 Gb/s speed and 5.2 dB modulation depth (f) 64 Gb/s speed and 4.7 dB modulation depth.

Table 1. Comparison with large FSR microring/disk modulators

Ref	Type	Radius (μm)	FSR (THz)	BW (GHz)	FSR × BW (THz × GHz)	Speed (Gb/s)
[4]	Adiabatic Ring	4	6.92	-	-	12.5
[5]	Interior Ridge Ring	2.5	5.3	-	-	30
[6]	Spoked Ring/Disk	Outer = 4.36 Inner = 3.05	3.2	20	64	20
[7,8]	MOSCAP Ring	1.5	8.5	< 7	<59.5	10
This Work	Ring	3.8	3.2	41	131.2	64

4. Conclusion

A high-performance, compact Si MRM with a radius of 3.8 µm and FSR of 3.2 THz is demonstrated. The modulator has a vertical junction design, operates at a bandwidth of 41 GHz with a high DC extinction ratio (> 20 dB), and has a modulation efficiency of 44 pm/V. The tradeoff between higher modulation efficiency and an increased RC time constant from the vertical junction is effectively mitigated with inductive peaking to achieve a 41 GHz bandwidth (at detuning of max modulation slope). The device is demonstrated to operate at 64 Gb/s NRZ (limited by instrument speed) with wide open eyes.

Acknowledgement

The work is funded by DARPA PIPES contract HR0011-19-3-0004. The views, opinions and/or findings expressed are those of the authors and should not be interpreted as representing the official views or policies of the Department of Defense or the U.S. Government.

The authors wish to thank Yoojin Ban of IMEC for her initial consultation on MRM designs. We also acknowledge Subharup Roy and Hanyi Ding of Global Foundries for their assistance in gathering test data and Kainoa Kekahuna of FormFactor for help with high-speed experiments. Alan Arakawa of AMD provided layout support for all PIC tape-outs.

5. References

[1] D. A. B. Miller, "Attojoule Optoelectronics for Low-Energy Information Processing and Communications," IEEE Journal of Lightwave Technology **35**, 346-396 (2017).

[2] Y. Tong et al., "An Experimental Demonstration of 160-Gbit/s PAM-4 Using a Silicon Micro-Ring Modulator," IEEE Photonics Technology Letters **32**, 125-128 (2020).

[3] Y. Zhang et al., "240 Gb/s optical transmission based on an ultrafast silicon microring modulator," Photon. Research **10**, 1127-1133 (2022).

[4] A. Biberman et al., "Adiabatic microring modulators," Opt. Express **20**, 29223– 29236 (2012).

[5] E. Timurdogan et al., "An interior-ridge silicon microring modulator," J. Lightw. Technol **31**, 3907–3914 (2013).

[6] K. Al Qubaisi et al., "Microring Modulators in a New Silicon Photonics-Optimized 45 nm Monolithic Electronics-Photonics SOI CMOS Platform," 2021 Conference on Lasers and Electro-Optics (CLEO), San Jose, CA, USA, 2021, pp. 1-2.

[7] H. Gevorgyan et al, "MOSCAP Ring Modulator with 1.5 µm Radius, 8.5 THz FSR and 30 GHz/V Shift Efficiency in a 45 nm SOI CMOS Process," 2021 Optical Fiber Communications Conference and Exhibition (OFC), San Francisco, CA, USA, 2021, pp. 1-3.

[8] H. Gevorgyan et al. "Miniature, highly sensitive MOSCAP ring modulators in co-optimized electronic-photonic CMOS." Photonics Research **10**, A1-A7 (2022).

[9] K. Giewont et al., "300-mm Monolithic Silicon Photonics Foundry Technology," IEEE Journal of Selected Topics in Quantum Electronics **25**, 1-11 (2019).

[10] H. -C. Kao et al., "Study of Electrical and Optical Peaking of Si Ring Modulators for Tailoring Modulation Band," IEEE Photonics Journal, **15**, 1-6 (2023).